ISSN 1070-4280, Russian Journal of Organic Chemistry, 2024, Vol. 60, No. 10, pp. 1991–1998. © Pleiades Publishing, Ltd., 2024.

Effect of Laterally Substituted Methoxy Group on the Mesomorphic Behavior of Novel Ester Derivatives

N. K. Baku[a],*, K. D. Ladva[b], A. Y. Cholera[a], and J. J. Travadi[c]

[a] *Department of Chemistry, Atmiya University, Rajkot, Gujarat, 360005 India*

[b] *Principal, Shree Manibhai Virani & Smt. Navalben Virani Science College (Autonomous), Rajkot, Gujarat, 360005 India*

[c] *Chemistry Department, Kamani Science College and Prataprai Arts College, Amreli, Gujarat, 365601 India*

**e-mail: nkbaku29@gmail.com*

Received March 28, 2024; revised April 11, 2024; accepted April 13, 2024

Abstract—To understand how molecular structure affects liquid crystal behavior with reference to the lateral methoxy group, a novel homologous series of liquid crystal derivatives was synthesized and analyzed. The homologous series consists of 12 derivatives (C_1–C_{16}), of which the first five homologs (C_1–C_5) are not liquid crystals, while the remaining homologs (C_6–C_{16}) are enantiotropically smectogenic liquid crystals without exhibiting the nematic phase. The average thermal stability of the smectic phase is 77.85°C, and the mesophase length ranges from 4 to 17°C. The molecular structures were verified by analytical and spectral data. The liquid crystal properties of the novel series were compared with those of structurally similar known homologous series. The transition temperatures were determined by an optical polarizing microscope equipped with a heating stage.

Keywords: liquid crystals, smectogenic, mesomorphism, DSC, ester

DOI: 10.1134/S1070428024100154

INTRODUCTION

In the initial stage of the liquid crystal history, Reinitzer investigated many liquid crystal phases [1]. A mesomorphic state is a particular state of matter that possesses crystal-like optical properties and the ability to flow like a liquid. Liquid crystals are important in various fields due to their dual nature, including soft matter nanotechnology, biotechnology, and microtechnology [2], liquid crystals for energy harvesters, micromachines, and soft robots [3], data storage and encryption [4], liquid crystal elastomers [5], sunlight-driven polymer actuators [6], photovoltaics [7], metal nanoparticles-doped liquid crystals, polymer-dispersed liquid crystals [8], sensor systems [9], and other fields.

To correlate the effects of molecular structure with the liquid crystal properties of substances, we decided to synthesize new liquid crystals by modifying the series obtained previously. We reversed the construction of the series in which the position of the lateral methoxy group and the unsaturated ethylene double bond changed so that the length-to-breadth ratio also changed. Among other factors, the molecular aromaticity, central groups, terminal groups, positions of the same or different functional groups in the phenyl ring or rings, geometrical shape, size, polarity, and polarizability can also affect the liquid crystalline property [10]. We have synthesized ester-linkage thermotropic liquid crystals in which the alkyl group is present at the terminal group and the lateral methoxy group is present at the left-hand side terminal phenyl ring at the adjacent position of the *n*-alkoxy group. The alkyl chain as a terminal group in any composition expands the mesomorphic characteristics and thermal stabilities of different mesophases [11]. The liquid crystalline properties are predominantly affected by the lateral methoxy group, as observed by Travadi et al. [12]. Likewise, research on laterally substituted methoxy groups has applications in the liquid crystal field [13, 14], and the liquid crystalline properties also depend on the length-to-breadth ratio [15]. These results have motivated us for the proposed research work which is planned to synthesize

Scheme 1.

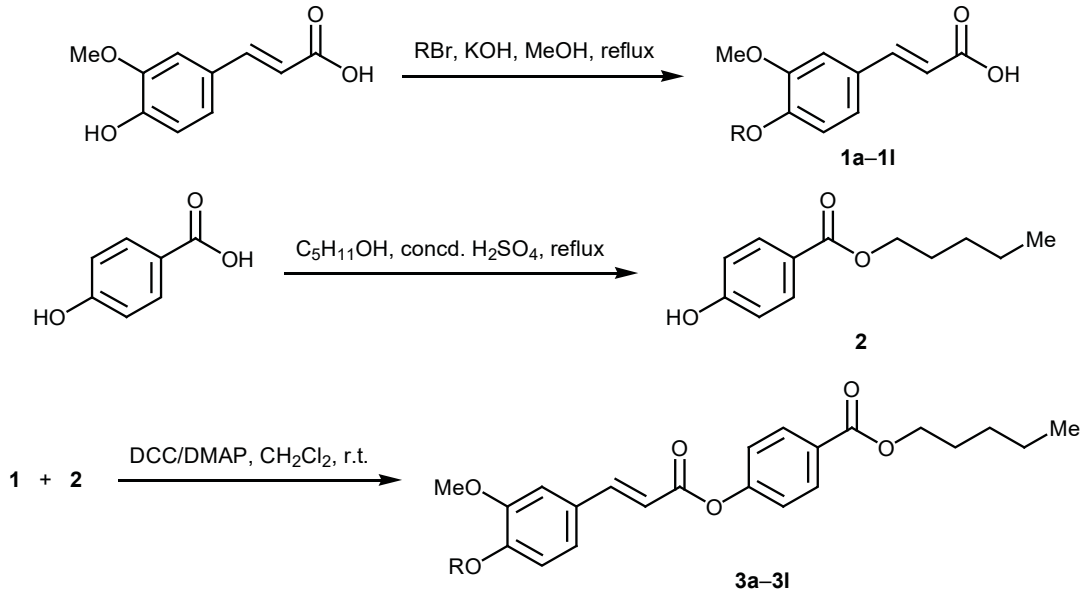

R = C_nH_{2n+1}; n = 1 (**a**), 2 (**b**), 3 (**c**), 4 (**d**), 5 (**e**), 6 (**f**), 7 (**g**), 8 (**h**), 10 (**i**), 12 (**j**), 14 (**k**), 16 (**l**).

novel ester derivatives of thermotropic liquid crystalline materials and study the effect of molecular structure on mesomorphic properties.

RESULTS AND DISCUSSION

A novel series of esters **3a**–**3l** were synthesized as illustrated in Scheme 1 by Steglich esterification of (*E*)-3-(4-alkoxy-3-methoxyphenyl)prop-2-enoic acids **1a**–**1l** with pentyl 4-hydroxybenzoate (**2**).

Mesomorphic behavior. The mesomorphic characteristics of the newly synthesized compounds were determined by polarizing optical microscopy (POM). The observed phase transition temperatures are given in Table 1, and the mesophase textures of representative compounds are shown in Fig. 1. In these studies, the heating and cooling rates were maintained at 10–12 deg/min.

The methoxy to pentyloxy homologs **3a**–**3e** are non-liquid crystalline compounds. Mesomorphic prop-

Table 1. Phase transition temperatures (°C) of compounds **3a**–**3l**

Compound no.	R	Smectic	Isotropic
3a	CH_3	–	128
3b	C_2H_5	–	119
3c	C_3H_7	–	127
3d	C_4H_9	–	100
3e	C_5H_{11}	–	92
3f	C_6H_{13}	65	82
3g	C_7H_{15}	70	85
3h	C_8H_{17}	62	71
3i	$C_{10}H_{21}$	71	78
3j	$C_{12}H_{25}$	81	88
3k	$C_{14}H_{29}$	63	73
3l	$C_{16}H_{33}$	65	69

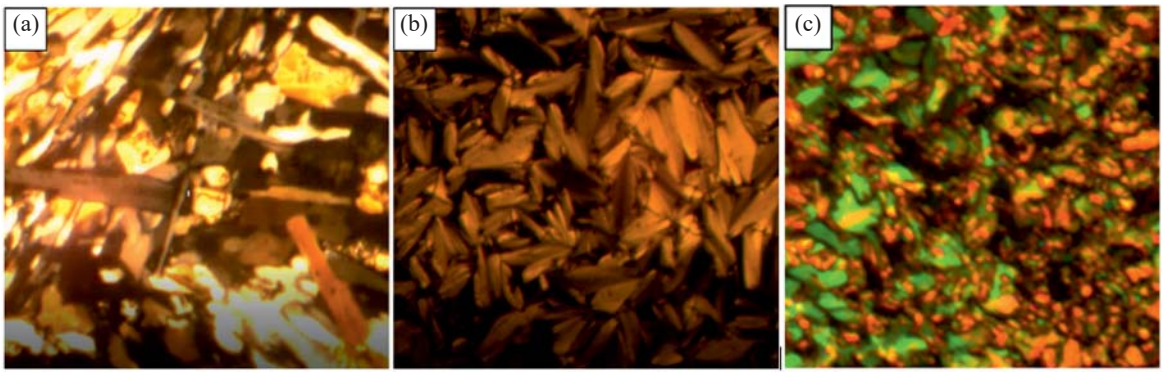

Fig. 1. Mesophase texture observed by POM: (a) smectic phase of compound **3f** at 60°C during the cooling cycle; (b) smectic phase of compound **3k** at 58°C during the cooling cycle; (c) smectic phase of compound **3j** at 81°C during the heating cycle.

erties emerge starting from hexyloxy derivative **3f** and continue up to hexadecyloxy derivative **3l** of the series in an enantiotropic way, showing only the smectic phase in the absence of nematic phase. Figure 2 shows the transition temperatures plotted versus the number of carbon atoms in the left side terminal *n*-alkyl chain.

The phase behavior of the series is represented by the transition curves shown in Fig. 2, which are obtained by linking similar or related points. The appropriate points are linked to obtain Cr-I/Cr-Sm as well as Sm-I transition curves. The Sm-I transition curve follows a rising-falling pattern up to C_{10} homologue **3i**, then rises for **3j** (C_{12}), and descends again up to **3l** (C_{16}). According to the phase diagram, the Cr-I/Cr-Sm transition curve follows a zigzag pattern of rising and falling. The length of the *n*-alkoxy terminal group affects the mesomorphic behavior of the series, while the rest of the molecule remains unchanged from homologue to homologue. The polarity and polarizability of the lateral electron-donating methoxy group adjacent to the terminal group of the left-hand side phenyl ring increases the length-to-breadth ratio. Appropriate intermolecular lateral attractions as a consequence of favorable molecular rigidity and flexibility promote mesophase formation from the C_6 to C_{16} homologs in an enantiotropic manner. The first five members of the series do not show mesophases due to their strong crystallizing tendency induced by inappropriately large anisotropic forces between molecules and lateral attractions. However, at appropriate temperatures, lamellar packing of molecules **3f**–**3l** (C_6–C_{16}) in their crystal lattices becomes possible, which continues at higher temperatures depending on favorable magnitudes of molecular stiffness and flexi-

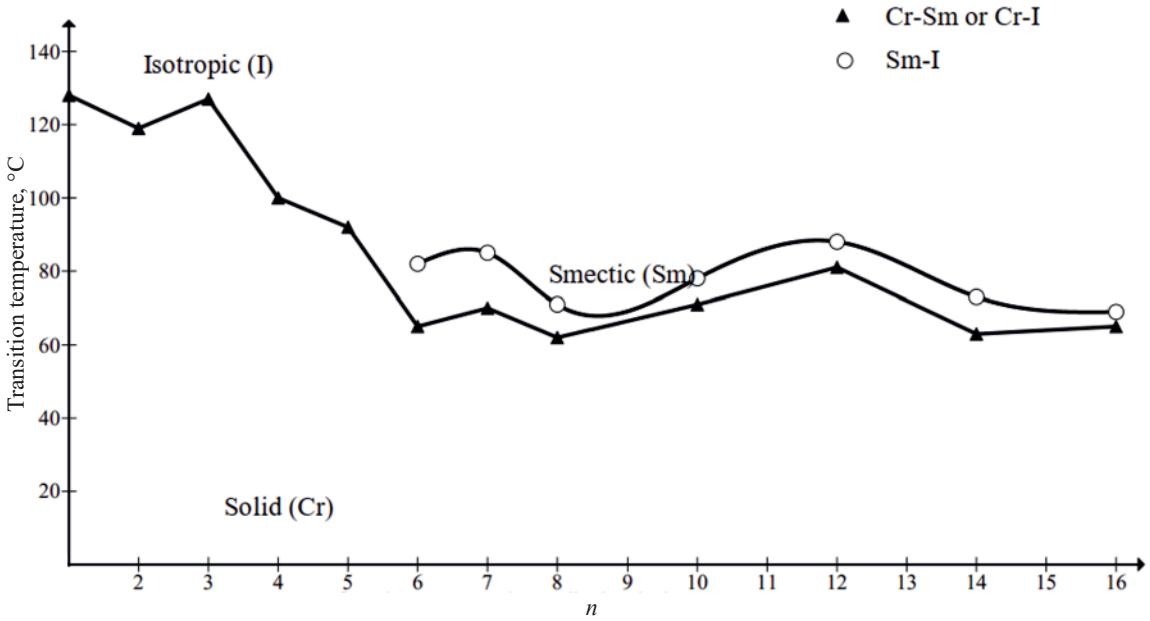

Fig. 2. Phase behavior of homologous series **3a**–**3l**.

bility until the isotropic temperature. The entire homologous series shows smectogenic behavior and the lack of nematic property. The absence of nematic properties is attributed to weaker end-to-end attractions, which hinder the formation of statistically parallel orientational order. The changes in mesomorphic behavior from one homolog to another in the same series are due to changes in molecular length caused by the successive addition of a methylene group to the left-hand terminal group. The permanent dipole moment over the long molecular axis, dipole–dipole interactions, electronic interactions, dispersion forces, etc., change accordingly. Thus, the changing pattern varies with the change in rigidity and flexibility, resulting in smectogenic mesomorphic properties.

DSC analysis. The thermal behavior of compounds **3f** (C_6) and **3k** (C_{14}) was studied by differential scanning calorimetry (Fig. 3). The DSC thermograms were recorded in both heating and cooling modes to determine the specific phase transition temperatures. The presence of two endothermic peaks indicated transitions from crystalline to smectic and from smectic to isotropic phases. For compound **3f**, the first endothermic peak was observed at 65°C under heating conditions, which indicated the presence of a smectic phase, while the second endothermic peak was observed at 82°C, which indicated the isotropic phase. The enthalpy of the system was estimated at 99.79 and 1.03 J/g. During the exothermic or cooling cycle, these two phase transition curves were also seen in reverse order. The compound showed isotropic behavior throughout the cooling process at 63°C, while the smectic transition occurred below this temperature, at 60°C, and the compound reverted to the crystalline state at 38°C. The system enthalpy was found to change in the cooling cycle from –5.91 to –119.48 J/g. For compound **3k**, the first endothermic peak was observed at 63°C under heating conditions due to the formation of smectic phase, and isotropic phase was formed at 73°C. On cooling conditions, the exothermic peaks were found at 58°C and under 40°C. The enthalpy changed in the heating cycle from 99.79 to 3.91 J/g, and in the cooling cycle, from –3.82 J/g.

Comparative study of Series 1 and Series X homologs. The mesomorphic properties of the new series (**3a**–**3l**; Series 1) were compared with those of structurally related homologous series **4a**–**4l** (Series X) [16] (Fig. 4).

Compounds **4** were synthesized by coupling of 4-alkoxybenzoic acids with *trans*-ferulic acid *n*-pentyl ester. Compounds **3a**–**3l** were obtained by coupling between different alkoxy derivatives of *trans*-ferulic acids and pentyl 4-hydroxybenzoate. Unlike Series X, the lateral methoxy group in Series 1 homologs is present at the right-hand-side benzene ring and is adjacent to the *n*-alkoxy group. Another noticeable change is that the α,β-unsaturated ester group in Series 1 compounds is located between the benzene rings, whereas in Series X, the double bond is present near the terminal ester group. These two major changes alter the molecular polarizability, the length-to-breadth ratio of homologues, and even the steric hindrance. These structural changes may result in a change in liquid crystalline properties from homologue to homologue and from series to series. Table 2 shows some liquid crystalline properties of Series 1 and Series X compounds. As seen in Table 2, the compounds of both series are predominantly smectogenic without a nematic phase. In both series, the smectogenic mesophase is observed starting from the C_6 homolog.

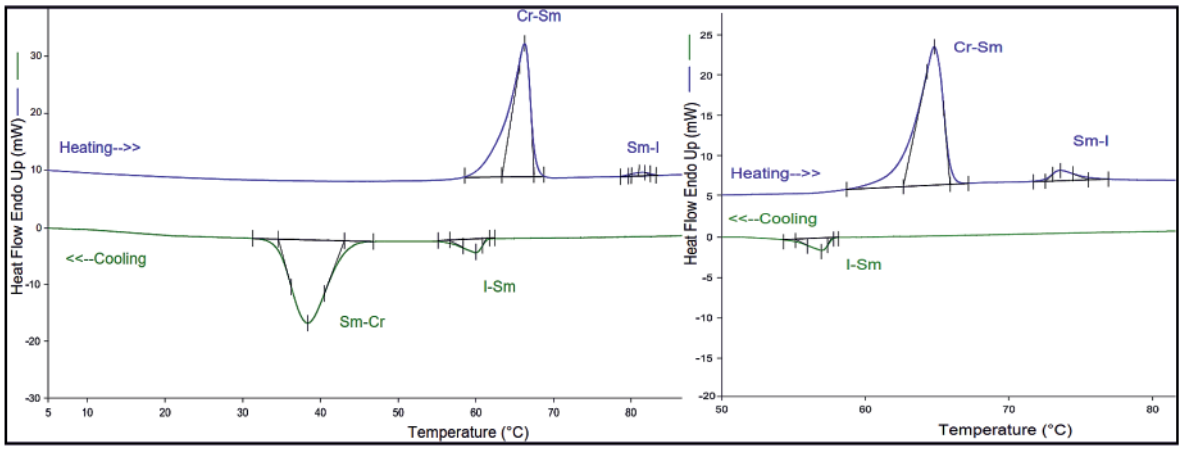

Fig. 3. DSC thermograms of compounds **3f** and **3k** during the heating and cooling cycles (heating/cooling rate 10 deg/min).

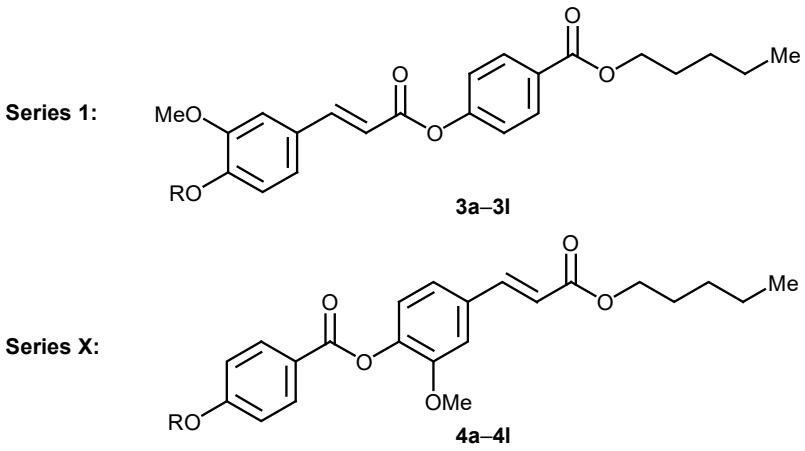

Fig. 4. Series 1 and Series X compounds.

Table 2. Average thermal stability of Series 1 and Series X compounds

Parameter	Series 1	Series X
Smectic–isotropic	77°C (C_6–C_{16})	81°C (C_6–C_{14})
Appearance of smectic phase	C_6	C_6
Mesophase length	4 to 17°C	9 to 31°C

The average thermal stability for Series 1 is 77.85°C, and for Series X, 81.8°C. This is the main difference resulting from the inversion of the structure. For Series X, the total mesophase length ranges from 9 to 31°C, which is larger than the total mesophase length range for Series 1 (4 to 17°C).

As follows from the molecular structures of Series 1 and Series X compounds, their horizontal axes have identical lengths, as they consist of two benzene rings and COO, OR, and CH=CH–COO units. The length-to-breadth ratio is lower in Series 1 than in Series X due to the changed positions of the lateral methoxy group and ethylene double bond. Thus, the positions of lateral substitution and CH=CH double bond are the main factors responsible for the presence or absence of nematic and smectic mesophases.

EXPERIMENTAL

The melting points were determined in open capillaries using a Tempo electrothermal device. The progress of reactions was monitored by thin-layer chromatography on precoated silica gel 60 F254 plates (Merck); spots were visualized under UV light at λ 254 or 365 nm or by treatment with iodine vapor. The IR spectra were recorded on a Shimadzu FT-IR spectrometer equipped with an ATR accessory. The ^{1}H NMR spectra were recorded with a Bruker Avance III spectrometer (400 MHz) in DMSO-d_6 using tetramethylsilane as an internal standard. The mass spectra were obtained on a Shimadzu GCMS QP2010 Ultra mass spectrometer using a direct inlet probe. All reactions were carried out under an ambient atmosphere. All chemicals were purchased from Loba, Molychem, SRL, and CDH and used without further purification. Enthalpies and transition temperatures were determined by differential scanning calorimetry (DSC) at a heating (cooling) rate of 10 deg/min using a Perkin Elmer thermal analyzer. The phase transition temperatures were also measured using a polarizing optical microscope attached to a Mettler FP82HT heating plate.

(*E*)-3-(4-Alkoxy-3-methoxyphenyl)prop-2-enoic acids 1a–1l (*general procedure*). A mixture of (*E*)-3-(4-hydroxy-3-methoxyphenyl)prop-2-enoic acid (0.1 mmol), corresponding alkyl halide (0.12 mmol), and potassium hydroxide (0.25 mmol) in 10 mL of methanol was refluxed for 3 to 4 h. A 10% aqueous solution of potassium hydroxide (20 mL) was then added, and the mixture was further refluxed for 2 h. The reflux time increased with increasing length of the alkyl chain. The mixture was cooled and acidified with dilute hydrochloric acid, and the precipitate was filtered off and recrystallized from ethanol or acetic acid [12, 17].

Pentyl 4-hydroxybenzoate (2). 4-Hydroxybenzoic acid (0.1 mmol) was added to 2 mL of anhydrous pentan-1-ol containing a catalytic amount of concentrated (98%) sulfuric acid. The mixture was refluxed in a water bath for 5 to 6 h, cooled, and poured into excess ice water (1 L or more). The solid product was filtered off, washed with a 4 N aqueous of sodium hydrogen carbonate and then with water, and recrystallized from distilled hexane [18, 19].

Pentyl (*E*)-4-{[3-(4-alkoxy-3-methoxyphenyl)-prop-2-enoyl]oxy}benzoates 3a–3l (*general procedure***).** *N*,*N*′-Dicyclohexylcarbodiimide (10 mmol) and a catalytic amount of 4-(dimethylamino)pyridine were added with stirring to a solution of (*E*)-3-(4-alkoxy-3-methoxyphenyl)prop-2-enoic acid **1a**–**1l** (10 mmol) and pentyl 4-hydroxybenzoate (**2**, 0.8 mmol) in 10 mL of methylene chloride. The mixture was stirred overnight, filtered, washed twice with a solution of sodium hydrogen carbonate, and concentrated. The residue was treated with hexane, and the product was isolated as white crystals [20–22].

Pentyl (*E*)-4-{[3-(3,4-dimetyloxyphenyl)prop-2-enoyl]oxy}benzoate (3a). Yield 75%. IR spectrum, ν, cm^{-1}: 619 (δCH_2), 854 (δC_6H_4-*p*), 2921 (CH_2), 1722, 1605, 1278 (C=O, C–O), 1515, 1452 (C–C_{arom}, HC=CH), 1119 (C–O), 1005 (CH=CH), 3052 (C–H_{arom}). Found, %: C 69.33; H 6.58. $C_{23}H_{26}O_6$. Calculated, %: C 69.38; H 6.53. *M* 398.

Pentyl (*E*)-4-{[3-(4-ethoxy-3-methoxyphenyl)-prop-2-enoyl]oxy}benzoate (3b). Yield 79%. IR spectrum, ν, cm^{-1}: 685 (δCH_2), 979 (δC_6H_4-*p*), 2921 (CH_2), 1721, 1602, 1263 (C=O, C–O), 1513, 1467 (C–C_{arom}, HC=CH), 1115 (C–O), 979 (CH=CH), 3025 (C–H_{arom}). Found, %: C 69.89; H 6.84. $C_{24}H_{28}O_6$. Calculated, %: C 69.87; H 6.88. *M* 412.

Pentyl (*E*)-4-{[3-(3-methoxy-4-propoxyphenyl)-prop-2-enoyl]oxy}benzoate (3c). Yield 78%. IR spectrum, ν, cm^{-1}: 657 (δCH_2), 789 (δC_6H_4-*p*), 2936 (CH_2), 1715, 1595, 1259 (C=O, C–O), 1515, 1452 (C=C_{arom}, HC=CH), 1016 (C–O), 912 (CH=CH), 3057 (C–H_{arom}). Found, %: C 70.40; H 7.709. $C_{25}H_{30}O_6$. Calculated, %: C 70.45; H 7.712. *M* 426.

Pentyl (*E*)-4-{[3-(4-butoxy-3-methoxyphenyl)-prop-2-enoyl]oxy}benzoate (3d). Yield 80%. IR spectrum, ν, cm^{-1}: 673 (δCH_2), 889 (δC_6H_4-*p*), 2926 (CH_2), 1722, 1595, 1298 (C=O, C–O), 1529 (C=C_{arom}, HC=CH), 1134 (C–O), 3007 (C–H_{arom}). ^{1}H NMR spectrum, δ, ppm: 0.87 t (6H, *J* = 6.8 Hz, CH_3), 1.30 m (4H, CH_2), 1.472 m (2H, CH_2), 1.73–1.72 m (4H, *J* = 6.4 Hz, CH_2), 3.84 s (3H, OCH_3), 4.31–4.30 m (2H, *J* = 6.4 Hz, OCH_2), 4.01 t (2H, *J* = 6.4 Hz, OCH_2), 8.04 d.d (2H, *J* = 6.8 Hz, H_{arom}), 7.36 d.d (2H, *J* = 8.4 Hz, H_{arom}), 7.02 d (1H, *J* = 8.4 Hz, H_{arom}), 7.31 d (1H, *J* = 8.4 Hz, H_{arom}), 7.45 s (1H, H_{arom}), 6.82 d (1H, *J* = 16 Hz, CH=CH), 7.83 d (1H, *J* = 16 Hz, CH=CH). Found, %: C 70.89; H 7.32. $C_{26}H_{32}O_6$. Calculated, %: C 70.91; H 7.38. *M* 440.

Pentyl (*E*)-4-({3-[3-methoxy-4-(pentyloxy)-phenyl]prop-2-enoyl}oxy)benzoate (3e). Yield 75%. IR spectrum, ν, cm^{-1}: 617 (δCH_2), 859 (δC_6H_4-*p*), 2925 (CH_2), 1725, 1607, 1279 (C=O, C–O), 1512, 1452 (C=C_{arom}, HC=CH), 1117 (C–O), 1004 (δCH=CH), 3056 (C–H_{arom}). Found, %: C 71.34; H 7.54. $C_{27}H_{34}O_6$. Calculated, %: C 71.38; H 7.59. *M* 454.

Pentyl (*E*)-4-({3-[4-(hexyloxy)-3-methoxy-phenyl]prop-2-enoyl}oxy)benzoate (3f). Yield 72%. IR spectrum, ν, cm^{-1}: 616 (δCH_2), 857 (δC_6H_4-*p*), 2925 (CH_2), 1723, 1605, 1281 (C=O, C–O), 1513, 1451 (C=C_{arom}, HC=CH), 1119 (C–O), 857 (δCH=CH), 3054 (C–H_{arom}). ^{1}H NMR spectrum, δ, ppm: 0.88 t [3H, *J* = 6.8 Hz, C**H**$_3$(CH_2)$_5$], 0.91 t [3H, C**H**$_3$(CH_2)$_4$], 1.30 m (8H, CH_2), 1.40 m (2H, CH_2), 1.73–1.71 m (4H, *J* = 6.8 Hz, CH_2), 3.826 s (3H, OCH_3), 4.29–4.27 m (2H, *J* = 7.6 Hz, OCH_2), 4.01 t (2H, *J* = 6.4 Hz, OCH_2), 8.03 d.d (2H, *J* = 8.4 Hz, H_{arom}), 7.37 d.d (2H, *J* = 8.4 Hz, H_{arom}), 7.01 d (1H, *J* = 8.4 Hz, H_{arom}), 7.31 d (1H, *J* = 8.4 Hz, H_{arom}), 7.45 s (1H, H_{arom}), 6.80 d (1H, *J* = 16 Hz, CH=CH), 7.82 d (1H, *J* = 16 Hz, CH=CH). Found, %: C 71.75; H 7.73. $C_{28}H_{36}O_6$. Calculated, %: C 71.77; H 7.74. *M* 468.

Pentyl (*E*)-4-({3-[4-(heptyloxy)-3-methoxyphenyl]prop-2-enoyl}oxy)benzoate (3g). Yield 73%. IR spectrum, ν, cm^{-1}: 615 (δCH_2), 859 (δC_6H_4-*p*), 2925 (CH_2), 1722, 1616, 1282 (C=O, C–O), 1513, 1452 (C=C_{arom}, HC=CH), 1179 (C–O), 1012 (δCH=CH), 3027 (C–H_{arom}). ^{1}H NMR spectrum, δ, ppm: 0.88 m (6H, CH_3), 1.26 m (6H, CH_2), 1.41 m (6H, CH_2), 1.75–1.73 m (4H, *J* = 6.8 Hz, CH_2), 3.84 s (3H, OCH_3), 4.33–4.31 m (2H, *J* = 6.8 Hz, OCH_2), 4.01 t (2H, *J* = 6.4 Hz, OCH_2), 8.05 d.d (2H, *J* = 8.8 Hz, H_{arom}), 7.38 d.d (2H, *J* = 8.4 Hz, H_{arom}), 7.02 d (1H, *J* = 8.4 Hz, H_{arom}), 7.33 d (1H, *J* = 8.8 Hz, H_{arom}), 7.45 s (1H, H_{arom}), 6.82 d (1H, *J* = 16 Hz, CH=CH), 7.83 d (1H, *J* = 16 Hz, CH=CH). Found, %: C 72.17; H 7.94. $C_{29}H_{38}O_6$. Calculated, %: C 72.19; H 7.97. *M* 482.

Pentyl (*E*)-4-({3-[3-methoxy-4-(octyloxy)phenyl]-prop-2-enoyl}oxy)benzoate (3h). Yield 75%. IR spectrum, ν, cm^{-1}: 616 (δCH_2), 853 (δC_6H_4-*p*), 2923, 2920 (CH_2), 1721, 1603, 1281 (C=O, C–O), 1513, 1451

(C=C_{arom}), 1119 (C–O), 1001 (δCH=CH), 3065 (C–H_{arom}). ^{1}H NMR spectrum, δ, ppm: 0.87 t [3H, *J* = 7.2 Hz, C**H**$_3$(CH$_2$)$_7$], 0.92 t [3H, *J* = 6.8 Hz, C**H**$_3$(CH$_2$)$_4$], 1.28 m (8H, CH_2), 1.42 m (6H, CH_2), 1.75 m (4H, *J* = 6.8 Hz, CH_2), 3.84 s (3H, OCH_3), 4.02 t (2H, *J* = 6.4 Hz, OCH_2), 4.31–4.28 m (2H, *J* = 6.4 Hz, OCH_2), 8.05 d.d (2H, *J* = 8.8 Hz, H_{arom}), 7.35 d.d (2H, *J* = 2 Hz, H_{arom}), 7.03 d (1H, *J* = 8.8 Hz, H_{arom}), 7.33 d (1H, *J* = 2 Hz, H_{arom}), 7.47 s (1H, *J* = 1.6 Hz, H_{arom}), 6.82 d (1H, *J* = 15.16 Hz, CH=CH), 7.84 d (1H, *J* = 14.8 Hz, CH=CH). Found, %: C 72.77; H 8.18. $C_{30}H_{40}O_6$. Calculated, %: C 72.55; H 8.12. *M* 496.

Pentyl (*E*)-4-({3-[4-(decyloxy)-3-methoxyphenyl]prop-2-enoyl}oxy)benzoate (3i). Yield 72%. IR spectrum, ν, cm^{-1}: 619 (δCH_2), 852 (δC_6H_4-*p*), 2919 (CH_2), 1718, 1602, 1276 (C=O, C–O), 1510, 1448 (C=C_{arom}, HC=CH), 1117 (C–O), 1007 (δCH=CH), 3057 (C–H_{arom}). Found, %: C 73.25; H 8.45. $C_{32}H_{44}O_6$. Calculated, %: C 73.26; H 8.48. *M* 524.

Pentyl (*E*)-4-({3-[4-(dodecyloxy)-3-methoxyphenyl]prop-2-enoyl}oxy)benzoate (3j). Yield 78%. IR spectrum, ν, cm^{-1}: 682 (δCH_2), 857 (δC_6H_4-*p*), 2919 (CH_2), 1771, 1601, 1261 (C=O, C–O), 1515, 1469 (C=C_{arom}, HC=CH), 1117 (C–O), 981 (δCH=CH), 3022 (C–H_{arom}). ^{1}H NMR spectrum, δ, ppm: 0.88 t [3H, *J* = 6.8 Hz, C**H**$_3$(CH$_2$)$_{11}$], 0.91 t [3H, C**H**$_3$(CH$_2$)$_4$], 1.30 m (8H, CH_2), 1.40 m (2H, CH_2), 1.73–1.71 m (4H, *J* = 6.8 Hz, CH_2), 3.83 s (3H, OCH_3), 4.29–4.27 m (2H, *J* = 7.6 Hz, OCH_2), 4.01 t (2H, *J* = 6.4 Hz, OCH_2), 8.03 d.d (2H, *J* = 8.4 Hz, H_{arom}), 7.37 d.d (2H, *J* = 8.4 Hz, H_{arom}), 7.00 d (1H, *J* = 8.4 Hz, H_{arom}), 7.31 d (1H, *J* = 8.4 Hz, H_{arom}), 7.45 s (1H, H_{arom}), 6.81 d (1H, *J* = 16 Hz, CH=CH), 7.82 d (1H, *J* = 16 Hz, CH=CH). Found, %: C 73.88; H 8.75. $C_{34}H_{48}O_6$. Calculated, %: C 73.83; H 8.79. *M* 552.

CONCLUSIONS

The novel homologous series of esters consisting of two phenyl rings connected through the CH=CH–COO group, terminal OAlk and $COOC_5H_{11}$ groups, and lateral methoxy group are smectogenic from C_6 to C_{16} with a low melting point. As compared to the previously synthesized homologous series, the new compounds showed lower thermal stability, similar smectic mesophase formation temperature, and lesser total mesophase length (temperature range). The sequential addition of methylene units to the left end of the *n*-alkoxy terminal group affects the mesomorphic properties of homologues within the same series. The width of the molecules of the new series is smaller compared to the previous series, but there is no significant change in the flexibility of homologue to homologue, so the nematic phase is not observed. The newly synthesized homologous series may be useful for studying binary systems, as well as for agricultural purposes [23, 24].

AUTHOR INFORMATION

N.K. Baku, ORCID: https://orcid.org/0000-0001-8872-4879

K.D. Ladva, ORCID: https://orcid.org/0000-0003-1090-8787

A.Y. Cholera, ORCID: https://orcid.org/0000-0001-6352-8257

ACKNOWLEDGMENTS

The authors are thankful to the management, principal, and Head of the Chemistry Department, Shree Manibhai Virani & Smt. Navalben Virani Science College (Autonomous) (Rajkot) and Kamani Science College & Prataprai Arts College (Amreli) for their valuable cooperation in facilitating the present research work. The authors are also grateful to the authorities of Saurashtra University and Atmiya University for analytical services.

FUNDING

This work was supported by ongoing institutional funding. No additional grants to carry out or direct this particular research were obtained.

CONFLICT OF INTEREST

The authors declare that they have no conflicts of interest.

SUPPLEMENTARY INFORMATION

The online version contains supplementary material available at https://doi.org/10.1134/S1070428024100154.

REFERENCES

1. Reinitzer, F., *Monatsh. Chem*., 1888, vol. 9, p. 421. https://doi.org/10.1007/BF01516710
2. Lagerwall, J.P. and Scalia, G., *Curr. Appl. Phys*., 2012, vol. 12, p. 1387. https://doi.org/10.1016/j.cap.2012.03.019
3. Wang, Y., Sun, J., Liao, W., and Yang, Z., *Adv. Mater*., 2022, vol. 34, p. 840. https://doi.org/10.1002/adma.202107840

4. Gao, J., Tian, M., He, Y., Yi, H., and Guo, J., *Adv. Funct. Mater*., 2022, vol. 32, article ID 2107145. https://doi.org/10.1002/adfm.202107145
5. Ula, S.W., Traugutt, N.A., Volpe, R.H., Patel, R.R., Yu, K., and Yakacki, C.M., *Liq. Cryst. Rev*., 2018, vol. 6, p. 78. https://doi.org/10.1080/21680396.2018.1530155
6. Jiang, Z.C., Xiao, Y.Y., Tong, X., and Zhao, Y., *Angew. Chem., Int. Ed*., 2019, vol. 58, p. 5332. https://doi.org/10.1002/anie.201900470
7. Khalid, M., Shanks, K., Ghosh, A., Tahir, A., Sundaram, S., and Mallick, T.K., *Renewable Energy*, 2021, vol. 164, p. 96. https://doi.org/10.1016/j.renene.2020.09.069
8. Ahmad, F., Luqman, M., and Jamil, M., *Mol. Cryst. Liq. Cryst*., 2021, vol. 731, p. 1. https://doi.org/10.1080/15421406.2021.195475
9. Bubnov, A., Cigl, M., Penkov, D., Otruba, M., Pociecha, D., Chen, H.H., and Hamplová, V., *Polymers*, 2021, vol. 13, article no. 2156. https://doi.org/10.3390/polym13132156
10. Travadi, J.J., *Int. J. Res. Appl. Sci. Eng. Technol*., 2018, vol. 6, p. 2164. https://doi.org/10.22214/ijraset.2018.3341
11. Zakaria, M.A., Alazmi, M., Katariya, K.D., El Kilany, Y., El Ashry, E.S.H., Jaremko, M., Hagar, M., and Mohammady, S.Z., *Crystals*, 2021, vol. 11, article no. 978. https://doi.org/10.3390/cryst11080978
12. Vadodaria, M.S., Ladva, K.D., Doshi, A.V., and Travadi, J.J., *Mol. Cryst. Liq. Cryst*,, 2016, vol. 624, p. 59. https://doi.org/10.1080/15421406.2015.1044158
13. Stojanović, M., Bubnov, A., Obadović, D. Ž., Hamplová, V., Cvetinov, M., and Kašpar, M., *Mater. Chem. Phys*., 2014, vol. 146, p. 18. https://doi.org/10.1016/j.matchemphys.2014.02.036
14. Alamro, F.S., Ahmed, H.A., Popoola, S.A., Altaleb, H.A., Al-Ola, A., and Gomha, K.A., *Crystals*, 2021, vol. 11, article no. 870. https://doi.org/10.3390/cryst11080870
15. Baku, N.K., Travadi, J.J., and Ladva, K., *Curr. Phys. Chem*., 2024, vol. 14, p. 20. https://doi.org/10.2174/1877946813666230809121625
16. Travadi, J.J., Vadodaria, M.S., Ladva, K.D., and Doshi, A.V., *Mol. Cryst. Liq. Cryst*., 2016, vol. 626, p. 21. https://doi.org/10.1080/15421406.2015.1106222
17. Dave, J.S. and Vora, R.A., *Liquid Crystals and Ordered Fluids*, Johnson, J.F. and Porter, R.S., Eds., New York: Springer, 1970, p. 477. https://doi.org/10.1007/978-1-4684-8214-0_38
18. Vogel, A.I., *Vogel's Textbook of Practical Organic Chemistry*, London: Longman Scientific & Technical: 1989, 5th ed.
19. Chauhan, M.L., Pandya, R.N., and Doshi, A.V., *Mol. Cryst. Liq. Cryst*., 2011, vol. 548, p. 228. https://doi.org/10.1080/15421406.2011.591664
20. Suthar, D.M., Doshi, A.A. and Doshi, A.V., *Mol. Cryst. Liq. Cryst*., 2013, vol. 577, p. 51. https://doi.org/10.1080/15421406.2013.785812
21. Bhoya, U.C., Vyas, N.N., and Doshi, A.V., *Mol. Cryt. Liq. Cryst*., 2012, vol. 552, p. 104. https://doi.org/10.1080/15421406.2011.604590
22. Patel, P.K., Patel, R.B., and Shah, R.R., *World Sci. News*, 2016, vol. 54, p. 202.
23. Balasubramaniam, V.M. and Sastry, S.K., *J. Food Eng*., 1995, vol. 26, p. 219. https://doi.org/10.1016/0260-8774(94)00055-e
24. Mao, C. and Heitschmidt, J., *Proc. SPIE*, 1999, vol. 3543, p. 172. https://doi.org/10.1117/12.336879

Publisher's Note. Pleiades Publishing remains neutral with regard to jurisdictional claims in published maps and institutional affiliations.

AI tools may have been used in the translation or editing of the article.